

**DETC2009-87494**

## VIBRATION MODES OF HELICAL PLANETARY GEARS

**Tugan Eritenel**

Mechanical Engineering Department  
The Ohio State University  
Columbus, Ohio 43210  
Email: eritenel.1@osu.edu

**Robert G. Parker\***

State Key Lab for Mechanical Systems and Vibration  
Univ. of Michigan-SJTU Joint Institute  
Shanghai Jiao Tong University  
Shanghai, China  
Email: parker.242@osu.edu

### ABSTRACT

This paper examines the vibration modes of single stage helical planetary gears in three dimensions with equally spaced planets. A lumped-parameter model is formulated to obtain the equations of motion. The gears and shafts are modeled as rigid bodies with compliant bearings at arbitrary axial locations on the shafts. A translational and a tilting stiffness account for the force and moment transmission at the gear mesh interface. The modal properties generalize those of two-dimensional spur planetary gears; there are twice as many degrees of freedom and natural frequencies due to the added tilting and axial motion. All vibration modes are categorized as planet, rotational-axial, and translational-tilting modes. The modal properties are shown to hold even for configurations that are not symmetric about the gear plane, due to, for example, shaft bearings not being equidistant from the gear plane. Computational modal analysis are performed to numerically verify the findings.

### INTRODUCTION

Knowledge of the modal properties of planetary gears is crucial for developing strategies to reduce vibration. Planetary gear dynamic models are developed in [1–4]. Lin and Parker show that two-dimensional, spur planetary gears with equally spaced [5] and diametrically opposed [6] planets possess well-defined modal properties. They report all vibration modes belong to one of three categories: 1) Planet modes where only the planets move, and their motions are scalar multiples of the arbitrarily

chosen first planet's motion. 2) Rotational modes where the central members (sun, carrier, and ring) rotate but do not translate. The planet motions are identical. 3) Translational modes with degenerate natural frequencies, where the central members translate but do not rotate. There are well-defined relations between the two independent vibration modes at each natural frequency. Kiracofe and Parker [7] prove that a similar categorization applies to compound planetary gears. Wu and Parker [8] prove the modal properties of spur planetary gears having elastically deformable ring gears.

These vibration mode characteristics are crucial in vibration suppression strategies using mesh phasing [2, 9, 10] and eigensensitivity analysis [11, 12] of planetary gears. Schlegel and Mard [10], Seager [2], and Hidaka et al. [13] state that the vibration of planetary gears is reduced by proper gear mesh phasing. Hidaka et al. [13] experimentally and Kahraman [14] computationally investigate the effectiveness of vibration suppression by planet mesh phasing. Kahraman [14] uses a three-dimensional lumped-parameter model for computations. Blankenship and Kahraman [15] illustrate how some harmonics of the transmission error excitation vanish by adjusting the mesh phasing. Based on the well-defined modal properties of planetary gears, Parker [16] explains how proper mesh phasing suppresses many resonances of translational and rotational modes from certain harmonics of mesh frequency. Ambarisha and Parker [17] explain the vibration suppression of planet modes from mesh phasing.

Finite element analysis is incorporated with elaborate gear contact analysis in [18–22] to capture the complex dynamic be-

---

\*Address all correspondence to this author.

havior of planetary gears. These studies enable computationally efficient analysis of complex planetary gears and survey the effects of design parameters on dynamic behavior.

Although the vibration modes of two-dimensional planetary gears have been studied, it remains to be seen what the vibration mode characteristics are for helical planetary gears with three-dimensional motion, a three-dimensional gear mesh interface, and the gear-shaft bodies supported by bearings at arbitrary locations along the shafts. A lumped parameter model is formulated to include the tilting and axial motions, thus including all six degrees of freedom for each gear/shaft body. A tilting mesh stiffness augments the gear mesh interface to produce the three-dimensional force and moment transmission.

This paper is based on the work of Eritenel and Parker [23]. The method is outlined by which [23] proves that helical planetary gears with equally spaced planets have exactly three types of vibration modes. The details of the proof is omitted for it is not possible to retain the mathematical intelligibility while containing them in the recommended length of this conference paper. Compared to two-dimensional spur gear models there are twice as many natural modes, and their properties are different. Unique properties of these vibration modes are given. Computational modal analysis of an example system with four and five planets is presented. The proof indicates that the modal properties hold for configurations that are asymmetric about the gear plane, such as when the bearings are not equidistant from the gears. A computational study of an example system with overhung planets is presented to confirm this finding.

## MODEL

The planetary gear model consists of three central members (the sun, ring, and carrier) and  $p$  planets. The gear bodies and the carrier are integrated with their supporting shafts, so that each gear/shaft is a single body. These combined gear/shaft bodies are each mounted on up to two bearings placed at arbitrary axial locations. The sun, ring, and carrier bearings are connected to ground while the planet bearings are connected to the carrier. The gear/shaft bodies and carrier are rigid; the compliant elements are the meshing gear teeth and bearings. Figure 1 depicts the model with the parameters defining the system geometry. The vibration amplitudes are small, so geometric nonlinearities are neglected.

The indexing conventions  $b = s, r, c, 1, \dots, p$  for the sun, ring, carrier, and the planets,  $h = s, r, c$  for the sun, ring, and carrier, and  $i = 1, 2, \dots, p$  for the planets are maintained throughout this study. There are  $2p$  gear meshes. Odd numbers are assigned to the sun-planet meshes, and even numbers are assigned to the ring-planet meshes.

The origin is at the undeflected position of the center of the sun. A right handed, orthonormal basis  $\{\mathbf{E}\} = \{\mathbf{E}_1, \mathbf{E}_2, \mathbf{E}_3\}$  rotates with the constant carrier angular speed  $\Omega_c$ . For the central members, translational coordinates  $x_h, y_h, z_h$  are assigned to translations along  $\mathbf{E}_1, \mathbf{E}_2$ , and  $\mathbf{E}_3$ , respectively. Similarly, angu-

lar coordinates  $\phi_h, \theta_h, \beta_h$  are assigned to small rotations about  $\mathbf{E}_1, \mathbf{E}_2$ , and  $\mathbf{E}_3$ , respectively. Translational coordinates for the planets  $x_i, y_i, z_i$  are measured from the undeflected position of the centers of the planets in the bases  $\{\mathbf{E}^i\} = \{\mathbf{E}_1^i, \mathbf{E}_2^i, \mathbf{E}_3^i\}$  that rotate with the carrier angular speed. The base vector  $\mathbf{E}_1^i$  is parallel to the line of action of the  $i^{\text{th}}$  sun-planet mesh deflections. Angular coordinates  $\phi_i, \theta_i, \beta_i$  for the planets are assigned to rotations about  $\mathbf{E}_1^i, \mathbf{E}_2^i$ , and  $\mathbf{E}_3^i$ , respectively. Body fixed bases for all the bodies  $\{\mathbf{e}^b\} = \{\mathbf{e}_1^b, \mathbf{e}_2^b, \mathbf{e}_3^b\}$  are adopted because the gear mesh deflection expressions are algebraically simpler in these bases.

Axial position quantities in Fig. 1(a) are measured from the datum position, which is at the center of the active facewidth and

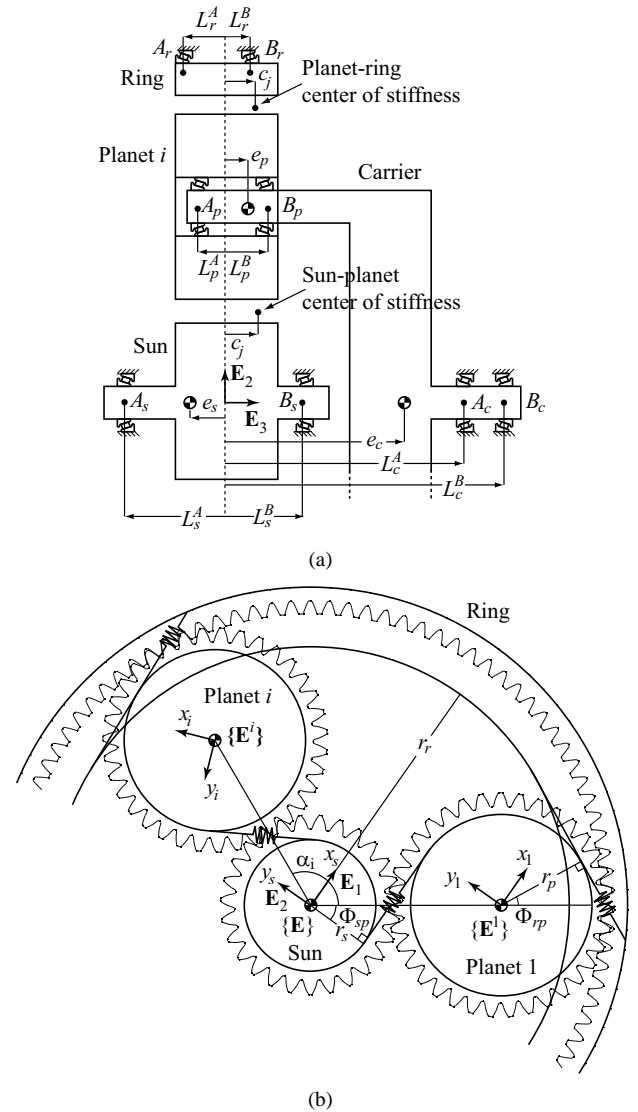
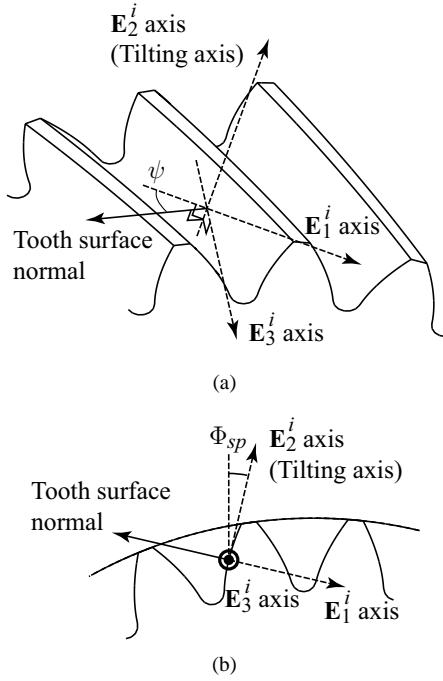


Figure 1. Coordinates and dimensions used in the planetary gear model.

denoted by the dashed line. Any inactive facewidth is treated as a part of the shaft. This setup allows arbitrary axial positioning of gears with different facewidths. Positive planet position angle  $\alpha_i$  is measured counter-clockwise from the arbitrarily chosen first planet.

Two linear springs, one translational and one tilting, model the gear mesh interface. The translational stiffness ( $k_j$ ) accounts for the transmitted force through the gear mesh. Its associated relative translational deflection ( $\delta_j$ ) is in the direction of the tooth surface normal. The tilting stiffness ( $\kappa_j$ ) accounts for the moment transmitted through the gear mesh. Its associated angular deflection is about an axis that is in the gear plane and perpendicular to both the line of action  $\mathbf{E}_1^i$  and the tooth surface normal. Figure 2 shows the line of action  $\mathbf{E}_1^i$ , the tooth surface normal, and the tilting axis  $\mathbf{E}_2^i$  for the  $i^{\text{th}}$  sun-planet mesh. These two deflections are calculated at a specified point along the facewidth, called the center of stiffness. The axial position of the center of stiffness is  $c_j$ . The translational stiffness, tilting stiffness, and center of stiffness can be reduced from gear tooth contact models, such as [24], averaged over a mesh cycle.



**Figure 2.** Tooth surface normal and the tilting axis for the  $i^{\text{th}}$  sun-planet mesh. The  $i^{\text{th}}$  planet gear is shown.  $\psi$  is the base helix angle, and  $\Phi_{sp}$  is the transverse operating pressure angle.

The equations of motion come from Lagrange's equations for unconstrained generalized coordinates. The kinetic and po-

tential energies are

$$T = \frac{1}{2} \sum_{b=1}^N \left( \boldsymbol{\omega}_b^T \mathbf{J}_b \boldsymbol{\omega}_b + \dot{\mathbf{r}}_b^T m_b \dot{\mathbf{r}}_b \right),$$

$$V = \frac{1}{2} \sum_{b=1}^N \left( \mathbf{d}_{A,b}^T \mathbf{K}_{A,b} \mathbf{d}_{A,b} + \mathbf{d}_{B,b}^T \mathbf{K}_{B,b} \mathbf{d}_{B,b} \right) + \frac{1}{2} \sum_{b=1}^N \left( \zeta_{A,b}^T \boldsymbol{\chi}_{A,b} \zeta_{A,b} + \zeta_{B,b}^T \boldsymbol{\chi}_{B,b} \zeta_{B,b} \right) + \frac{1}{2} \sum_{j=1}^{2p} \left( k_j \delta_j^2 + \kappa_j \gamma_j^2 \right), \quad (1)$$

where  $N = p + 3$  is the number of bodies,  $\boldsymbol{\omega}_b$  is the angular velocity,  $m_b$  is the mass,  $\mathbf{J}_b$  is the inertia tensor,  $\dot{\mathbf{r}}_b$  is the velocity vector,  $\mathbf{d}_{A,b}$  is the translational bearing deflection vector,  $\zeta_{A,b}$  is the angular bearing deflection vector,  $\mathbf{K}_{A,b}$  is the bearing stiffness matrix for translation, and  $\boldsymbol{\chi}_{A,b}$  is the bearing stiffness matrix for rotation. The translational gear mesh deflection is  $\delta_j$ ; the angular (tilting) gear mesh deflection is  $\gamma_j$ ; the translational gear mesh stiffness is  $k_j$ ; and, the tilting gear mesh stiffness is  $\kappa_j$ .

The angular velocity of the  $b^{\text{th}}$  body in its corotational basis  $\{\mathbf{e}^b\}$  is

$$\boldsymbol{\omega}_b = \left[ \dot{\phi}_b - \theta_b (\dot{\beta}_b + \Omega_b) \right] \mathbf{e}_1^b + \left[ \dot{\theta}_b + \phi_b (\dot{\beta}_b + \Omega_b) \right] \mathbf{e}_2^b + \left[ \dot{\beta}_b + \Omega_b - \phi_b \dot{\theta}_b \right] \mathbf{e}_3^b, \quad (2)$$

where  $\Omega_b$  is the constant kinematic rotation speed. The inertia tensor for each body in its principal axes is  $\mathbf{J}_b = \text{diag} [J_b^x, J_b^y, J_b^z]$  with constant components. All gears are axisymmetric, so  $J_b^y = J_b^x$ . The velocity vectors of the central members ( $h = s, r, c$ ), and planets ( $i = 1, 2, \dots, p$ ), are

$$\dot{\mathbf{r}}_h = [\dot{x}_h - \Omega_c y_h] \mathbf{E}_1 + [\dot{y}_h + \Omega_c x_h] \mathbf{E}_2 + \dot{z}_h \mathbf{E}_3 \quad (3)$$

$$\dot{\mathbf{r}}_i = [\dot{x}_i - \Omega_c (y_i - r_s - r_p)] \mathbf{E}_1 + [\dot{y}_i + \Omega_c (x_i + \tan \Phi_{sp} (r_s + r_p))] \mathbf{E}_2 + \dot{z}_i \mathbf{E}_3, \quad (4)$$

where  $\Phi_{sp}$  and  $\Phi_{rp}$  are the sun-planet and ring-planet transverse operating pressure angles.

The bearings are attached to the points  $A_b$  and  $B_b$  on the left and right sides of the  $b^{\text{th}}$  body, respectively. The bearing deflection vectors for central members at point  $A_h$  is

$$\mathbf{d}_{A,h} = [x_h - (e_h + L_h^A) \theta_h] \mathbf{E}_1 + [(e_h + L_h^A) \phi_h + y_h] \mathbf{E}_2 + z_h \mathbf{E}_3, \quad (5)$$

where  $e_h$ ,  $L_h^A$ , and  $L_h^B$  are the axial positions of the mass centers, bearings  $A_h$ , and bearings  $B_h$  of the central members. The bearing deflection vectors at point  $B_h$  follow similarly. Positive values of  $e_h$  and  $L_h^A$  are measured from the datum along  $\mathbf{E}_3$ , and positive values of  $L_h^B$  are measured from the datum along  $-\mathbf{E}_3$ . This sign convention is chosen so that for positive  $L_h^A$  and  $L_h^B$  the gears are in between the bearings. The bearing deflection vector for the planets is the relative position between the point that is on the carrier and the point that is on the planet shaft. The bearing deflection vector for the planets at point  $A_i$  is

$$\begin{aligned} \mathbf{d}_{A,i} = & \left\{ [\theta_c(e_s + L_p^A) - x_c] \cos \alpha_i - [y_c + \phi_c(e_s + L_p^A)] \sin \alpha_i \right. \\ & \left. - \beta_c(r_p + r_s) + x_i - \theta_i(e_p + L_p^A) \right\} \mathbf{E}_1^i \\ & + \left\{ [x_c - \theta_c(e_s + L_p^A)] \sin \alpha_i - [y_c + \phi_c(e_s + L_p^A)] \cos \alpha_i \right. \\ & \left. - \tan \Phi_{sp} \beta_c(r_p + r_s) + y_i + \phi_i(e_p + L_p^A) \right\} \mathbf{E}_2^i \\ & + \left\{ [-\tan \Phi_{sp} \phi_c(r_s + r_p) + \theta_c(r_s + r_p)] \sin \alpha_i \right. \\ & \left. + [\tan \Phi_{sp} \theta_c(r_s + r_p) + \phi_c(r_s + r_p)] \cos \alpha_i + z_i - z_c \right\} \mathbf{E}_3^i, \end{aligned} \quad (6)$$

The bearing deflection for point  $B_i$  is similar, and it can be found in [23] Eq. (8).

The angular bearing deflection vector is the relative angular displacements of the connected bodies. The angular bearing deflection vectors for the central members and planets at points  $A_h$  and  $A_i$  are

$$\zeta_{A,h} = \phi_h \mathbf{E}_1 + \theta_h \mathbf{E}_2 + \beta_h \mathbf{E}_3, \quad (7)$$

$$\begin{aligned} \zeta_{A,i} = & [\phi_i - \theta_c \sin \alpha_i - \phi_c \cos \alpha_i] \mathbf{E}_1^i + [\theta_i - \theta_c \cos \alpha_i \\ & + \phi_c \sin \alpha_i] \mathbf{E}_2^i + [\beta_i - \beta_c] \mathbf{E}_3^i. \end{aligned} \quad (8)$$

The angular bearing deflection vectors at points  $B_h$  and  $B_i$  are identical to Eqs. (7) and (8) for rigid shafts.

The bearings are isotropic in the  $\mathbf{E}_1 - \mathbf{E}_2$  plane. There is no coupling between different directions. For all bodies the bearing stiffness matrix for translation is  $\mathbf{K}_{A,b} = \text{diag} [k_b^A, k_b^A, k_b^{Az}]$ , and the bearing stiffness matrix for rotation is  $\chi_{A,b} = \text{diag} [\kappa_b^A, \kappa_b^A, \kappa_b^{Az}]$ , where the equality of stiffness in the two in-plane translation directions is evident (and similarly for rotation). These stiffness components are in the  $\{\mathbf{E}\}$  basis for the central members and in the  $\{\mathbf{E}^i\}$  basis for each of the planets.

The translational gear mesh deflection  $\delta_j$  is the relative compressive deflection at the center of stiffness in the direction normal to the tooth surface. The translational gear mesh deflection

for the sun-planet meshes ( $j = 1, 3, 5, \dots, 2p - 1$ ) is

$$\begin{aligned} \delta_j = & \left\{ [(e_s - c_j)\phi_s + y_s] \cos \psi \right. \\ & \left. + r_s [\theta_s - \phi_s \tan \Phi_{sp}] \sin \psi \right\} \sin \alpha_i \\ & + \left\{ [x_s - (e_s - c_j)\theta_s] \cos \psi \right. \\ & \left. + r_s [\phi_s + \theta_s \tan \Phi_{sp}] \sin \psi \right\} \cos \alpha_i \\ & + [(e_p - c_j)\theta_i + r_s \beta_s + r_p \beta_i - x_i] \cos \psi \\ & + [z_i - z_s + r_p(\phi_i + \theta_i \tan \Phi_{sp})] \sin \psi, \end{aligned} \quad (9)$$

where  $\psi$  is the base helix angle, and the center of stiffness for a gear mesh in the axial direction measured from the datum is  $c_j$ . The reader is referred to [23] Eq. (12) for the translational gear mesh deflection of the ring-planet meshes. The angular gear mesh deflection  $\gamma_j$  for the sun-planet meshes is

$$\gamma_j = \phi_s \sin \alpha_i - \theta_s \cos \alpha_i + \theta_i, \quad j = 1, 3, 5, \dots, 2p - 1, \quad (10)$$

The angular deflection for the ring-planet meshes can be found in [23] Eq. (14).

Lagrange's equations of motion are obtained following substitution of Eqs. (2) through (10) (including the expressions omitted in this paper) into the energy expressions in Eq. (1). In matrix form they are

$$\mathbf{M}\ddot{\mathbf{q}} + \mathbf{K}\mathbf{q} = \mathbf{f}, \quad (11)$$

$$\mathbf{q} = (\mathbf{q}_s, \mathbf{q}_r, \mathbf{q}_c, \mathbf{q}_1, \dots, \mathbf{q}_p), \quad (12)$$

$$\mathbf{q}_b = (\phi_b, \theta_b, \beta_b, x_b, y_b, z_b), \quad b = s, r, c, 1, \dots, p.$$

The diagonal inertia matrix  $\mathbf{M}$  is

$$\mathbf{M} = \text{diag}(\mathbf{M}_s, \mathbf{M}_r, \mathbf{M}_c, \mathbf{M}_1, \dots, \mathbf{M}_i, \dots, \mathbf{M}_p), \quad (13)$$

where an individual block is given by  $\mathbf{M}_b = \text{diag}(J_b^x, J_b^x, J_b^z, m_b, m_b, m_b)$ . Only certain blocks of the stiffness matrix  $\mathbf{K}$  are populated due to the geometric configuration of planetary gears. The  $6N \times 6N$  matrix has the form

$$\mathbf{K} = \begin{bmatrix} \mathbf{K}_s & \mathbf{0} & \mathbf{0} & \mathbf{K}_{s,1} & \mathbf{K}_{s,2} & \dots & \mathbf{K}_{s,p} \\ & \mathbf{K}_r & \mathbf{0} & \mathbf{K}_{r,1} & \mathbf{K}_{r,2} & \dots & \mathbf{K}_{r,p} \\ & & \mathbf{K}_c & \mathbf{K}_{c,1} & \mathbf{K}_{c,2} & \dots & \mathbf{K}_{c,p} \\ & & & \mathbf{K}_1 & \mathbf{0} & \dots & \mathbf{0} \\ & & & & \mathbf{K}_2 & \dots & \mathbf{0} \\ & & & & & \ddots & \vdots \\ & & & & & & \mathbf{K}_p \end{bmatrix}_{n \times n}, \quad (14)$$

where the total number of degrees of freedom is  $n = 6N$ . The  $6 \times 6$  sub-matrices  $\mathbf{K}_h$ , and  $\mathbf{K}_{h,i}$  are expanded in the following section. The individual elements of these sub-matrices and of  $\mathbf{K}_i$  are given in the appendix of [23]. The high-speed effects that arise from the constant kinematic rotation fall outside the scope of this study, so  $\Omega_c = 0$  is specified. Consequently, the gyroscopic matrix, centripetal acceleration matrix, and centripetal acceleration vector, which are given in [23], are omitted here.

If one considers motion  $\mathbf{y} = \mathbf{q} - \mathbf{q}_e$  about the steady configuration  $\mathbf{q}_e$  defined by  $\mathbf{K}\mathbf{q}_e = \mathbf{f}$ , where  $\mathbf{f}$  is the constant external loading vector, the governing equation is

$$\mathbf{M}\ddot{\mathbf{y}} + \mathbf{K}\mathbf{y} = \mathbf{f}_d(t), \quad (15)$$

where  $\mathbf{f}_d(t)$  is the zero-mean, dynamic external loading vector.

## MODAL ANALYSIS

The eigenvalue problem is

$$(\mathbf{K} - \lambda\mathbf{M})\mathbf{q} = 0 \quad (16)$$

with natural frequencies  $\sqrt{\lambda}$ . The vibration modes are divided into  $6 \times 1$  sub-vectors as

$$\mathbf{q} = (\mathbf{v}_s, \mathbf{v}_r, \mathbf{v}_c, \mathbf{v}_1, \dots, \mathbf{v}_p). \quad (17)$$

The system is tuned, that is, all sun-planet and ring-planet mesh stiffnesses, and their centers of stiffnesses, are identical among all planets; the planet bearing stiffnesses, the axial locations of the planet bearings, and the planet inertias are the same for all planets. Regardless of planet spacing, the stiffness and inertia sub-matrices satisfy

$$\begin{aligned} \mathbf{K}_h = & \Upsilon_h \sum_{i=1}^p \sin \alpha_i + \mathbf{R}\Upsilon_h\mathbf{R}^T \sum_{i=1}^p \cos \alpha_i + \Theta_h \sum_{i=1}^p \sin^2 \alpha_i \\ & + \mathbf{R}\Theta_h\mathbf{R}^T \sum_{i=1}^p \cos^2 \alpha_i + \Xi_h \sum_{i=1}^p \sin \alpha_i \cos \alpha_i + \Psi_h, \end{aligned} \quad (18)$$

$$\mathbf{R} = \begin{bmatrix} 0 & 1 & 0 & 0 & 0 & 0 \\ -1 & 0 & 0 & 0 & 0 & 0 \\ 0 & 0 & 1 & 0 & 0 & 0 \\ 0 & 0 & 0 & 0 & 1 & 0 \\ 0 & 0 & 0 & -1 & 0 & 0 \\ 0 & 0 & 0 & 0 & 0 & 1 \end{bmatrix}, \quad (19)$$

$$\mathbf{K}_i = \mathbf{K}_j, \mathbf{M}_i = \mathbf{M}_j, \quad i, j = 1, 2, \dots, p, \quad (20)$$

$$\mathbf{K}_{h,i} = \Lambda_h \sin \alpha_i + \mathbf{R}\Lambda_h \cos \alpha_i + \Gamma_h. \quad (21)$$

Individual elements of  $\Upsilon_h$ ,  $\Theta_h$ ,  $\Xi_h$ ,  $\Psi_h$ ,  $\Lambda_h$ , and  $\Gamma_h$  are given in [23].

## Computational Observation of Vibration Modes

An example planetary gear is analyzed with four and five equally spaced planets to expose the modal properties. The operating transverse pressure angle of sun-planet and ring-planet meshes are  $\Phi_{sp} = \Phi_{rp} = 21.3$  deg. Base helix angle on the sun is  $\psi = 28.5$  deg right handed. The sun-planet translational mesh stiffness is  $k_j = 1.76 \times 10^9$  N-m. The ring-planet translational mesh stiffness is  $k_j = 3.54 \times 10^9$  N-m. The sun-planet tilting mesh stiffness is  $\kappa_j = 35.9 \times 10^3$  N-m, The ring-planet tilting mesh stiffness is  $\kappa_j = 36 \times 10^3$  N-m. Axial distance of bearings are  $L_b^A = L_b^B = 20$  mm for all bodies except the planets. The planet bearing positions are varied from ( $L_p^A = 20$  mm,  $L_p^B = 20$  mm), in which case the planets are simply supported, to ( $L_p^A = -40$  mm,  $L_p^B = 80$  mm), in which case the planets are overhung. For the sun and carrier, the radial and axial bearing stiffnesses are  $k_h^A, k_h^B = 0.5 \times 10^9$  N/m, and the tilting bearing stiffnesses are nil. Rotation of the carrier is constrained by setting the rotational stiffness to  $9 \times 10^{10}$  N-m. The ring is practically fixed by setting all bearing stiffnesses to  $5 \times 10^9$  including nominal rotation with appropriate units. The sun and planets are free to rotate. The inertias are as follows:  $m_s = 0.3$  kg,  $J_s^x = 0.005$  kg-m<sup>2</sup>,  $J_s^z = 0.01$  kg-m<sup>2</sup>,  $m_p = 0.2$  kg,  $J_p^x = 0.005$  kg-m<sup>2</sup>,  $J_p^z = 0.01$  kg-m<sup>2</sup>,  $m_c = 0.5$  kg,  $J_s^x = 0.004$  kg-m<sup>2</sup>,  $J_s^z = 0.008$  kg-m<sup>2</sup>. Some natural frequencies and their corresponding mode types are given in Table 1.

**Table 1. Natural frequencies [Hz] below 3000 Hz and mode types of the planetary gear system with four and five planets. R-A: Rotational-axial mode, T-T: Translational-tilting mode, P: Planet mode. Natural frequency multiplicity is not shown.**

Four Planets		Five Planets	
Nat. freq. [Hz]	Mode type	Nat. freq. [Hz]	Mode type
395	T-T	369	T-T
431	R-A	416	R-A
963	P	963	P
1085	T-T	1045	T-T
1132	R-A	1171	R-A
1477	T-T	1475	T-T
1537	R-A	1538	R-A
1537	P	1538	P
1568	P	1569	P
1601	R-A	1611	R-A
1734	T-T	1773	T-T

The vibration modes exhibit distinctive characteristics. Figures 3, 4, and 5 show two of each three vibration modes of the sample system with four planets. Regardless of the system pa-

rameters the modal deflections of certain gears are zero, or there is a relation between certain degrees of freedom such that not all modal deflections are independent. Based on these features, all vibration modes are categorized as planet, rotational-axial, and translational-tilting modes. These three types bear some similarities to those described by Lin and Parker [5], but they have important differences.

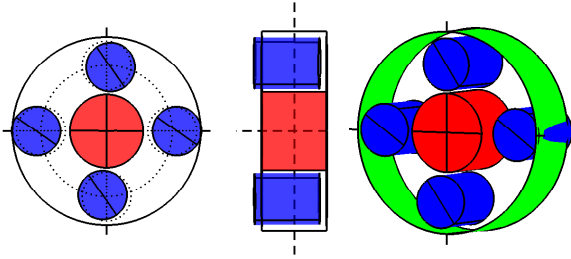


Figure 3. A planet mode at 963 Hz of the planetary gear system with four equally spaced planets. Angular and translational displacements are scaled independently to emphasize behavior.

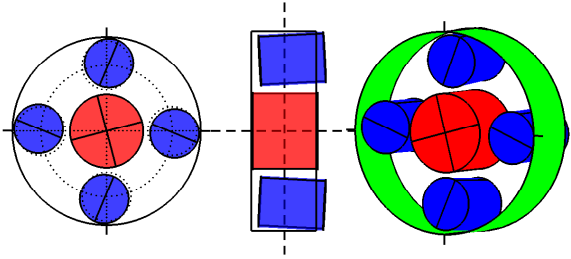


Figure 4. A rotational-axial mode at 431 Hz of the planetary gear system with four equally spaced planets. Angular and translational displacements are scaled independently to emphasize behavior.

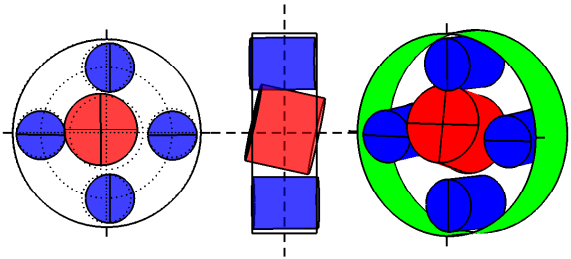


Figure 5. A translational-tilting mode at 1734 Hz of the planetary gear system with four equally spaced planets. Angular and translational displacements are scaled independently to emphasize behavior.

In a planet mode shown in Fig. 3 all central members are stationary. This is given by

$$\mathbf{v}_h = \mathbf{0}, \quad h = s, r, c. \quad (22)$$

The planets move in all six degrees of freedom, and their motions are related to that of the arbitrarily selected first planet by

$$\mathbf{v}_i = w_i \mathbf{v}_1, \quad i = 2, \dots, p, \quad (23)$$

where the  $w_i$  are constants. Planet modes are observed only when there are four or more planets ( $p \geq 4$ ). The natural frequency multiplicity is  $p - 3$ .

There are 12 rotational-axial modes for systems with more than two planets. The natural frequency multiplicity is one. From the computed eigenvectors (in Fig. 4, for example) the central members rotate and translate axially, but they do not tilt or translate in-plane. The modal deflection of any central member is of the form

$$\mathbf{v}_h = (0, 0, \beta_h, 0, 0, z_h). \quad (24)$$

The planets move in all degrees of freedom, and their modal deflections are identical to one another as given by

$$\mathbf{v}_1 = \mathbf{v}_2 = \dots = \mathbf{v}_p. \quad (25)$$

There are 12 pairs of translational-tilting modes with natural frequency multiplicity of two for systems with three or more planets. In both modes of a translational-tilting mode pair, shown in Fig. 5, the central members only translate in-plane and tilt but do not rotate or translate axially. The modal deflections of any central member for a pair of vibration modes have the form

$$\begin{aligned} \mathbf{v}_h &= (\phi_h, \theta_h, 0, x_h, y_h, 0), \quad \mathbf{w}_h = (\theta_h, -\phi_h, 0, y_h, -x_h, 0) \\ &\rightarrow \mathbf{w}_h = \mathbf{R} \mathbf{v}_h, \quad h = s, r, c. \end{aligned} \quad (26)$$

The planets move in all six degrees of freedom. Their motions are such that the modal deflections of any planet can be found from the modal deflections of the arbitrarily selected first planet using

$$\begin{pmatrix} \mathbf{v}_i \\ \mathbf{w}_i \end{pmatrix} = \begin{bmatrix} \cos \alpha_i \mathbf{I} & \sin \alpha_i \mathbf{I} \\ -\sin \alpha_i \mathbf{I} & \cos \alpha_i \mathbf{I} \end{bmatrix} \begin{pmatrix} \mathbf{v}_1 \\ \mathbf{w}_1 \end{pmatrix}, \quad i = 2, \dots, p, \quad (27)$$

where  $\mathbf{I}$  is the  $6 \times 6$  identity matrix.

## Analytical Characterization of Vibration Modes

The observed properties of the different types of vibration modes are proved for general systems with three or more planets in [23]. This section gives the method and summarizes the steps of the proof, but some details are omitted.

The proof consists of constructing a candidate vibration mode (for each mode type) based on the observed characteristics and substituting it into the eigenvalue problem Eq. (16). Showing that the eigenvalue problem is satisfied ensures that the proposed vibration mode is truly a system vibration mode.

The critical point for all three mode types is that some elements of the candidate vibration mode are linearly dependent on others. A candidate vibration mode is partitioned as

$$\mathbf{q} = (\mathbf{u}, \mathbf{q}^*), \quad \mathbf{q}^* = \mathbf{Y}\mathbf{u}, \quad (28)$$

where the vector  $\mathbf{u}$  contains elements regarded as independent, and the vector  $\mathbf{q}^*$  is the vector of dependent elements calculated from  $\mathbf{u}$ . How the modal deflections are partitioned between  $\mathbf{u}$  and  $\mathbf{q}^*$  as well as the matrix  $\mathbf{Y}$  differ for each of the three mode types, but all three types can be expressed in this general form with known  $\mathbf{Y}$ . The three specific cases are discussed subsequently.

Substitution of the candidate vibration mode from Eq. (28) into the eigenvalue problem Eq. (16) results in

$$\begin{bmatrix} \mathbf{A} & \mathbf{B}^T \\ \mathbf{B} & \mathbf{E} \end{bmatrix} \begin{pmatrix} \mathbf{u} \\ \mathbf{q}^* \end{pmatrix} = \lambda \begin{bmatrix} \mathbf{M}_u & \mathbf{0} \\ \mathbf{0} & \mathbf{M}_l \end{bmatrix} \begin{pmatrix} \mathbf{u} \\ \mathbf{q}^* \end{pmatrix}, \quad (29)$$

where  $\mathbf{A}$ ,  $\mathbf{B}$ , and  $\mathbf{E}$  are partitioned matrices of  $\mathbf{K}$ ;  $\mathbf{M}_u$  and  $\mathbf{M}_l$  are partitioned matrices of the diagonal  $\mathbf{M}$ . Substitution of  $\mathbf{q}^* = \mathbf{Y}\mathbf{u}$  into Eq. (29) expresses the upper row in the form of a reduced eigenvalue problem

$$(\mathbf{A} + \mathbf{B}^T \mathbf{Y})\mathbf{u} = \lambda \mathbf{M}_u \mathbf{u}. \quad (30)$$

This equation contains all the necessary information to find the natural frequencies and vibration modes of the type of vibration mode under consideration because the remaining elements  $\mathbf{q}^*$  of  $\mathbf{q}$  are found from Eq. (28). *For such a mode to indeed be a system mode, however, the lower row of Eq. (29) must hold, which is given by*

$$\mathbf{B}\mathbf{u} + \mathbf{E}\mathbf{q}^* = \lambda \mathbf{M}_l \mathbf{q}^*. \quad (31)$$

*This equation is crucial for the rest of this paper.*

In what follows, we prove that Eq. (31) holds for appropriately selected candidate vibration modes of the form Eq. (28) constructed for each of the three mode types. In each case,  $\mathbf{u}$

is calculated by Eq. (30). In this process, the algebraic properties of the stiffness and inertia matrices are pivotal. Furthermore, we show that this process yields *all* of the system modes, that is, *every* mode is either a rotational-axial, translational-tilting, or planet mode. The construction of matrices  $\mathbf{Y}$ ,  $\mathbf{B}$ ,  $\mathbf{E}$ ,  $\mathbf{A}$ ,  $\mathbf{M}_u$ , and  $\mathbf{M}_l$ , are dictated by the partitioning of each candidate mode type by Eq. (28).

With the stipulations that the planets are equally spaced and the system is tuned, the following developments do not depend on, and are therefore valid for arbitrary values of, system parameters such as gear radii, pressure and helix angles, locations and stiffnesses of the bearings, mesh stiffnesses, and so on.

The decomposition of the candidate planet mode according to Eqs. (22), (23), and (28) is

$$\mathbf{u} = w_1 \mathbf{v}_1, \quad \mathbf{q}^* = (\mathbf{0}, \mathbf{0}, \mathbf{0}, w_2 \mathbf{v}_1, \dots, w_p \mathbf{v}_1), \quad (32)$$

where the zero vectors are  $6 \times 1$ . We specify without loss of generality that  $w_1 \mathbf{v}_1 \neq \mathbf{0}$ , that is, at least the arbitrarily selected first planet deflects. The modal deflections of other planets are a scalar multiple of the modal deflections of the first planet as given in Eq. (23), although the  $w_i$  ( $i = 1, \dots, p$ ) are yet to be determined. Substitution of matrices  $\mathbf{B}$ ,  $\mathbf{E}$ ,  $\mathbf{M}_l$ , and Eq. (32) into Eq. (31), and use of Eqs. (18)-(21) yields

$$\sum_{i=1}^p w_i \sin \alpha_i = 0, \quad \sum_{i=1}^p w_i \cos \alpha_i = 0, \quad \sum_{i=1}^p w_i = 0. \quad (33)$$

and

$$\mathbf{K}_1 \mathbf{v}_1 = \lambda \mathbf{M}_1 \mathbf{v}_1. \quad (34)$$

Equation (33) can be solved for  $p - 3$  solutions for  $p \geq 4$  [8, 17]. Each solution gives a non-trivial set of  $w_i$ ,  $i = 1, \dots, p$ , and this set can be scaled by an arbitrary constant. Equation (34) is identical to the reduced eigenvalue problem, which is found by substitution of  $\mathbf{A}$ ,  $\mathbf{B}$ ,  $\mathbf{Y}$ , and  $\mathbf{M}_u$  into Eq. (30).

Thus, every mode of the form Eq. (32), defined by Eqs. (22) and (23) constructed from  $\mathbf{v}_1$  and a set of  $w_i$ , satisfies the full eigenvalue problem Eq. (16). The reduced  $6 \times 6$  eigenvalue problem Eq. (34) yields six planet mode eigenvalues regardless of the number of planets. For each of the six eigensolution pairs  $(\lambda, \mathbf{v}_1)$  one can construct  $p - 3$  ( $p \geq 4$ ) eigenvectors of the full system using the solution sets for the  $w_i$  from Eq. (33). Hence, each of the six planet mode natural frequencies has multiplicity  $p - 3$ . There are no planet modes if there are less than four planets because no set of  $w_i$  satisfying Eq. (33) can be found.

The candidate rotational-axial mode described by Eqs. (24), (25) is decomposed according to Eq. (28). Equal planet spacing

yields

$$\sum_{i=1}^p \sin i\alpha = 0, \quad \sum_{i=0}^p \cos i\alpha = 0, \quad (35)$$

from [25]. Substitution of  $\mathbf{B}$ ,  $\mathbf{E}$ ,  $\mathbf{M}_l$ , and  $\mathbf{q}^*$ , and use of Eqs. (18)-(21), and (35) confirms that Eq. (31) is satisfied using  $\mathbf{u}$  found from the reduced eigenvalue problem. The reduced eigenvalue problem is found by substitution of  $\mathbf{A}$ ,  $\mathbf{B}$ ,  $\mathbf{Y}$ , and  $\mathbf{M}_u$  into Eq. (30).

Thus, every rotational-axial mode  $\mathbf{q}$  defined by Eqs. (24) and (25), where each  $\mathbf{u}$  is determined from the reduced eigenvalue problem in Eq. (30) satisfies the full eigenvalue problem Eq. (16). In the rotational-axial mode case, Eq. (30) is a  $12 \times 12$  eigenvalue problem, so the reduced eigenvector  $\mathbf{u}$  has 12 elements. Therefore, there are 12 rotational-axial modes. Because each reduced eigenvector  $\mathbf{u}$  produces only one rotational-axial mode, each rotational-axial mode has a distinct natural frequency.

The candidate pair of translational-tilting modes given by the relations Eqs. (26) and (27) satisfy the eigenvalue problem Eq. (16) with the same eigenvalue. This is expressed as

$$(\mathbf{K} - \lambda\mathbf{M})\mathbf{q}_1 = \mathbf{0}, \quad (\mathbf{K} - \lambda\mathbf{M})\mathbf{q}_2 = \mathbf{0}. \quad (36)$$

Any linear combination of  $\mathbf{q}_1$  and  $\mathbf{q}_2$  also satisfies the full eigenvalue problem with the same eigenvalue. To apply the formulation in Eqs. (30) and (31), we stack the two expressions in Eq. (36) into a single block-diagonal matrix eigenvalue problem of dimension  $12(p+3)$  with eigenvector

$$\mathbf{q} = (\mathbf{q}_1, \mathbf{q}_2). \quad (37)$$

This eigenvalue problem is partitioned to give Eq. (29). One finds using [25] that

$$\sum_{i=1}^p \sin^2 i\alpha = \frac{p}{2}, \quad \sum_{i=1}^p \cos^2 i\alpha = \frac{p}{2}, \quad \sum_{i=1}^p \sin i\alpha \cos i\alpha = 0, \quad (38)$$

for equally spaced planets  $\alpha = 2\pi/p$ . Substitutions of  $\mathbf{B}$ ,  $\mathbf{E}$ ,  $\mathbf{M}_l$ , and  $\mathbf{q}^*$  into Eq. (31), and use of Eqs. (18)-(21), (26), (27), and (38) confirms that Eq. (31) is satisfied for the candidate translational-tilting mode for  $\mathbf{u}$  calculated from the reduced eigenvalue problem. The reduced eigenvalue problem is found by substitution of  $\mathbf{A}$ ,  $\mathbf{B}$ ,  $\mathbf{Y}$ , and  $\mathbf{M}_u$  into Eq. (30).

The foregoing analysis confirms that the degenerate mode pair  $\mathbf{q}_1$  and  $\mathbf{q}_2$  defined by Eqs. (26) and (27) each satisfy Eq. (16) with the same eigenvalue. The natural frequency multiplicity is two because one can exchange the letters  $\mathbf{v}$  and  $\mathbf{w}$  in Eqs. (26) and (27) with no change to any subsequent matrices or results. As a result, there are exactly 12 pairs of translational-tilting modes with twice repeated natural frequencies.

## Discussion

A helical planetary gear with  $p$  equally spaced planets and six degrees of freedom per component has  $18 + 6p$  degrees of freedom. There are six planet modes with natural frequency multiplicity  $p - 3$  (i.e.,  $6(p - 3)$  modes) provided  $p \geq 4$ . There are 12 rotational-axial modes with distinct natural frequencies; there are 24 translational-tilting modes (i.e., 12 degenerate mode pairs with natural frequency multiplicity two). Thus, all  $18 + 6p$  vibration modes have been accounted for. No other mode type is possible.

The only restrictions that the proof needs are the tuned system assumption and equal planet spacing. These restrictions are confined to the plane of the planetary gear. Parameter variations that do not disturb these stipulations have no effect on the properties of the vibration modes. There are no restrictions on the parameters that define the system in the axial direction. Therefore, contrary to intuition, the described mode types hold for configurations that are not symmetric about the plane of the gears, such as:

1. The bearings at opposite ends of a given gear-shaft body have different stiffness properties. An example is tapered roller bearings at one end and spherical roller bearings at the other end.
2. The bearings on a given gear-shaft body are at different distances from the gear plane; both bearings are on the same side of the gear plane; or, there is only one bearing. An example of such a configuration would be overhung gears and/or carrier. An example is analyzed in the next section.
3. The mass centers of the various gear-shaft bodies are at different axial positions.
4. The contact pattern is off-centered at the gear meshes. This may be due to, for example, lead modifications and deflection of the system under load. Note, however, that the sun-planet contact patterns must be the same at each planet (and the same for the ring-planet meshes).

These four items destroy symmetry about the gear plane, but the modal properties hold for these configurations and any combination thereof.

## RESULTS

The planets in the example system with four planets are supported by two bearings at points  $A_p$  and  $B_p$  at both ends of the gears  $L_p^A = 20$  mm,  $L_p^B = 20$  mm. Keeping the distance between the bearings same, the planet bearings are moved axially along  $\mathbf{E}_3$  until  $L_p^A = -40$  mm,  $L_p^B = 80$  mm. At  $L_p^A = -20$  mm,  $L_p^B = 60$  mm, the planets become overhung from their supporting shafts that connects them to the carrier. The natural frequencies of the system up to 3000 Hz are plotted in Fig. 6. The change in some natural frequencies is of practical interest. Natural frequencies of different mode types cross each other, but

veering [26] is observed among the natural frequencies of the same modes types.

The natural frequencies of the example planetary gear system with four and five planets are shown in Table 1. The natural frequency multiplicity of the translational-tilting modes is two, and the natural frequency multiplicity of the planet modes is two when there are five planets. The torque on the sun is increased from 200 N-m to 250 N-m for the system with five planets, so that the load that each planet carries is the same. The number of planets affect the rotational-axial and translational-tilting mode natural frequencies, but not the planet mode natural frequencies. This is because the reduced eigenvalue problems for the former two mode types include the number of planets as a parameter, but the reduced eigenvalue problem of the planet modes are independent of number of planets.

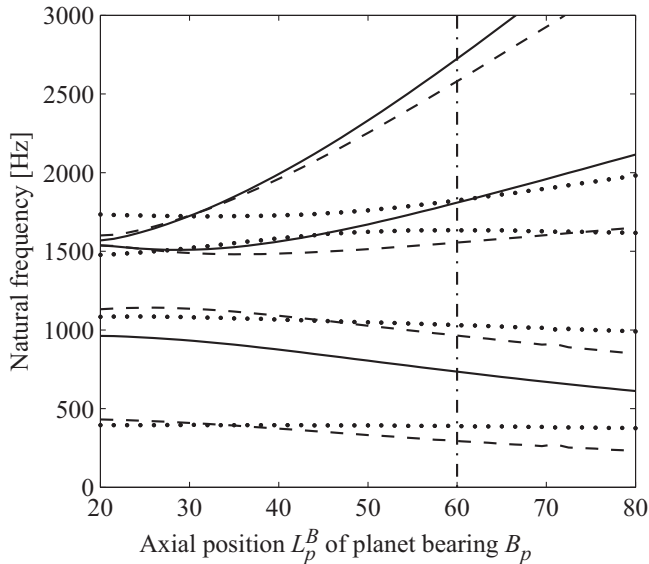


**Figure 6. Natural frequencies versus the axial position of the planet bearing  $B$ . Both bearings ( $A_p, B_p$ ) are moved out from the gear plane keeping the distance between them equal (40 mm). Initial planet bearing positions are ( $L_p^A = 20$  mm,  $L_p^B = 20$  mm). Final planet bearing positions are ( $L_p^A = -40$  mm,  $L_p^B = 80$  mm). The dash-dot line marks when the planets become overhung. Solid line: planet modes, dashed line: rotational-axial modes, dots: translational-tilting modes.**

## CONCLUSIONS

We prove that there are exactly three types of vibration modes of any tuned single-stage helical planetary gear system with equally spaced planets. The helical planetary gear system is represented by a three-dimensional lumped parameter model that allows for six degrees of freedom per gear-shaft body supported

by bearings at arbitrary axial positions. All vibration modes belong to one of these three types, described below:

1. Planet modes: Only the planets have modal deflection. Each planet's modal deflection is a known scalar multiple of any other planet's modal deflection. The central members do not move. There are six planet mode sets, where each set consists of  $p - 3$  degenerate (for  $p > 4$ ) modes having the same natural frequency. Planet modes exist only for systems with four or more planets ( $p \geq 4$ ).
2. Rotational-axial modes: The central members rotate and move axially but do not tilt or translate. The modal deflection of the planets are identical. There are 12 rotational-axial modes with distinct natural frequencies.
3. Translational-tilting modes: The central members tilt and translate in-plane but do not rotate or move axially. The modal deflections of all planets are related to one another according to Eq. (27). There are 12 pairs of degenerate translational-tilting modes with natural frequency multiplicity two.

Modal analysis of an example system with four and five planets confirm the conclusions regarding the natural frequency multiplicity described above.

The classification of the vibration modes persists for systems that are not symmetric about the plane of the planetary gear because the proof is valid for arbitrary values of all parameters that lead to such asymmetry. Computational modal analysis is performed for a system with varying planet axial bearing positions, so that the planets originally simply supported become overhung. The mode types are preserved. The veering-crossing pattern is one that is expected from the characterization of modes; same types of modes veer, but different types of modes can cross.

## REFERENCES

- [1] Cunliffe, F., Smith, J. D., and Welbourn, D. B., 1974. "Dynamic tooth loads in epicyclic gears". *Journal of Engineering for Industry*, **5**(95), May, pp. 578–584.
- [2] Seager, D. L., 1975. "Conditions for the neutralization of excitation by the teeth in epicyclic gearing". *Journal of Mechanical Engineering Science*, **17**(5), pp. 293–298.
- [3] Botman, M., 1976. "Epicyclic gear vibrations". *Journal of Engineering for Industry*, Aug., pp. 811–815.
- [4] August, R., and Kasuba, R., 1986. "Torsional vibrations and dynamic loads in a basic planetary gear system". *Journal of Vibration, Acoustics, Stress, and Reliability in Design*, **108**(3), July, pp. 348–353.
- [5] Lin, J., and Parker, R. G., 1999. "Analytical characterization of the unique properties of planetary gear free vibration". *Journal of Vibration and Acoustics*, **121**(3), July, pp. 316–321.
- [6] Lin, J., and Parker, R. G., 2000. "Structured vibration characteristics of planetary gears with unequally spaced

- planets”. *Journal of Sound and Vibration*, **233**(5), June, pp. 921–928.
- [7] Kiracofe, D. R., and Parker, R. G., 2007. “Structured vibration modes of general compound planetary gear systems”. *Journal of Vibration and Acoustics*, **129**(1), Feb., pp. 1–16.
- [8] Wu, X., and Parker, R. G., 2008. “Modal properties of planetary gears with an elastic continuum ring gear”. *Journal of Applied Mechanics*, **75**(3), May, pp. 1–10.
- [9] Lin, J., and Parker, R. G., 2004. “Mesh phasing relationships in planetary and epicyclic gears”. *Journal of Mechanical Design*, **126**, Mar., pp. 365–370.
- [10] Schlegel, R. G., and Mard, K. C., 1967. “Transmission noise control approaches in helicopter design”. In ASME Design Engineering Conference, no. 67-DE-58.
- [11] Lin, J., and Parker, R. G., 1999. “Sensitivity of planetary gear natural frequencies and vibration modes to model parameters”. *Journal of Sound and Vibration*, **228**(1), Nov., pp. 109–128.
- [12] Guo, Y., and Parker, R. G., 2008. “Sensitivity of general compound planetary gear natural frequencies and vibration modes to modal parameters”. *Journal of Vibration and Acoustics*(Submitted).
- [13] Hidaka, T., Terauchi, Y., and Nagamura, K., 1979. “Dynamic behavior of planetary gear (6th report, influence of meshing-phase)”. *Bulletin of JSME*, **22**(169), July, pp. 1026–1033.
- [14] Kahraman, A., 1993. “Planetary gear train dynamics”. *Journal of Mechanical Design*, **116**(3), Sept., pp. 713–720.
- [15] Kahraman, A., and Blankenship, G. W., 1994. “Planet mesh phasing in epicyclic gear sets”. In International Gearing Conference, pp. 99–104.
- [16] Parker, R. G., 2000. “A physical explanation for the effectiveness of planet phasing to suppress planetary gear vibration”. *Journal of Sound and Vibration*, **236**, Sept., pp. 561–573.
- [17] Ambarisha, V. K., and Parker, R. G., 2006. “Suppression of planet mode response in planetary gear dynamics through mesh phasing”. *Journal of Vibration and Acoustics*, **128**(2), Apr., pp. 133–142.
- [18] Saada, A., and Velex, P., 1995. “An extended model for the analysis of the dynamic behavior of planetary trains”. *Journal of Mechanical Design*, **117**(2), June, pp. 241–247.
- [19] Abousleiman, V., and Velex, P., 2006. “A hybrid 3d finite element/lumped parameter model for quasi-static and dynamic analyses of planetary/epicyclic gear sets”. *Mechanism and Machine Theory*, **41**(6), June, pp. 725–748.
- [20] Ambarisha, V. K., and Parker, R. G., 2007. “Nonlinear dynamics of planetary gears using analytical and finite element models”. *Journal of Sound and Vibration*, **302**(3), May, pp. 577–595.
- [21] Parker, R. G., Agashe, V., and Vijayakar, S. M., 2000. “Dynamic response of a planetary gear system using a finite element/contact mechanics model”. *Journal of Mechanical Design*, **122**(3), Sept., pp. 304–310.
- [22] Bahk, C.-J., and Parker, R. G., 2008. “Nonlinear dynamics of planetary gears with equal planet spacing”. *Journal of Computational and Nonlinear Dynamics*(Submitted).
- [23] Eritenel, T., and Parker, R. G., 2009. “Modal properties of three-dimensional helical planetary gears”. *Journal of Sound and Vibration*. DOI:10.1016/j.jsv.2009.03.002, (In press).
- [24] Velex, P., and Maatar, M., 1996. “A mathematical model for analyzing the influence of shape deviations and mounting errors on gear dynamic behavior”. *Journal of Sound and Vibration*, **191**(5), Apr., pp. 629–660.
- [25] Gradshteyn, I. S., and Ryzhik, I. M., 1980. *Table of integrals, series, and products*. Academic Press, New York.
- [26] Lin, J., and Parker, R. G., 2001. “Natural frequency veering in planetary gears”. *Mechanics of Structures and Machines*, **29**(4), pp. 411–429.